Locating the QCD critical endpoint from Lee-Yang edge singularities using multi-point Padé approximations

K. Zambello[1] D. A. Clarke[2] J. Goswami[2] C. Schmidt[2]
S. Singh[3] F. Di Renzo[4] P. Dimopoulos[4]

[1] University of Pisa and INFN [2] University of Bielefeld
[3] University of Bonn [4] University of Parma and INFN

Trento, 08/09/2025

Introduction

QCD phase diagram

- Goal: we want to investigate the critical points in the QCD phase diagram
- We can think of at least three critical regions:

  (1) The Roberge-Weiss transition region

  (2) The chiral transition region

  (3) The region around the critical endpoint of QCD

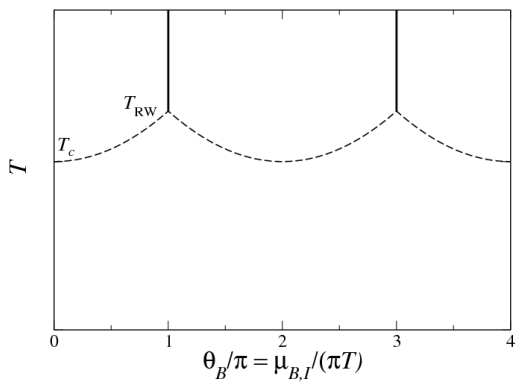

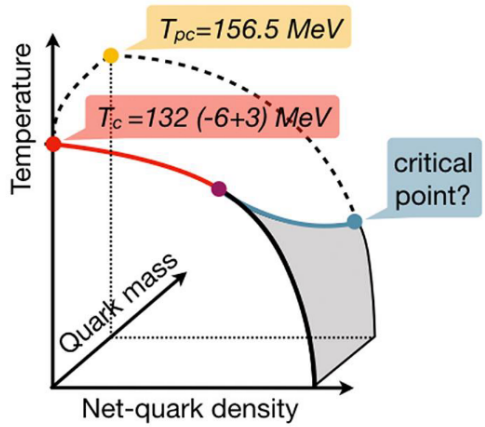

Fig. from Phys.Rev. D 93, 74504 (2016)

- More broadly, we aim to investigate the singularities of QCD in the complex μ-plane.

Introduction

Yang-Lee edge singularities

- There is a deep connection between phase transitions and the singularities in the complex plane.

The free energy has a branch cut on the imaginary axis for the symmetry breaking field h. The branch point is known as Yang-Lee edge singularity.

[Yang, Lee (1952)]

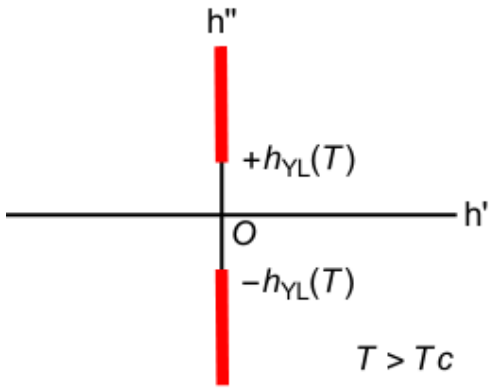

Fig. from New J. Phys. 19, 083009 (2017)

- Why are YLE singularities useful?

(1) If for $T \to T_c$ the YLE singularities end up on real axis this signals the presence of a physical phase transition

(2) At $T \neq T_c$ the presence of a YLE singularities determines a finite radius of convergence

- Strategy: find the location of critical points by tracking the location of the YLEs as a function of the thermodynamical parameters.

Introduction

The multi-point Padé method

- How do we get the information that we need from lattice data?

  Because of the sign problem we cannot directly explore regions at real (or even complex) chemical potentials.

- In our approach:

  (1) We perform simulations at imaginary μ

  (2) We calculate the Taylor coefficients of a given observable

  (3) We merge the results using multi-point Padé approximants

  We can extract information about the singularities of the observable by studying the uncanceled poles of the rational approximants.

- This Padé resummation scheme is a combination of the Taylor expansion and analytic continuation methods.

  Multi-point vs single-point Padé: replace the need for expensive high order Taylor coefficients with cheaper low order Taylor coefficients at multiple points.

- We look for a function of the form

$$R_{n,m}(\mu) = \frac{p_n(\mu)}{q_m(\mu)} = \frac{a_0 + a_1\mu + a_2\mu^2 + \ldots + a_n\mu^n}{1 + b_1\mu + b_2\mu^2 + \ldots + b_m\mu^m}$$

  that matches the Taylor coefficients of the observable.

- Multi-point Padé: we determine a_i, b_i by imposing

$$\partial^j_{\mu^j} R_{n,m}(\mu^{(k)}) = \partial^j_{\mu^j} \langle O \rangle(\mu^{(k)})$$

This yields a nonlinear system of eqs, but the problem can be linearized

$$\begin{cases} p_n(\mu^{(k)}) = \langle O \rangle(\mu^{(k)}) q_m(\mu^{(k)}) \\ p_n'(\mu^{(k)}) = \langle O \rangle'(\mu^{(k)}) q_m(\mu^{(k)}) + \langle O \rangle(\mu^{(k)}) q_m'(\mu^{(k)}) \\ p_n''(\mu^{(k)}) = \langle O \rangle''(\mu^{(k)}) q_m(\mu^{(k)}) + 2\langle O \rangle'(\mu^{(k)}) q_m'(\mu^{(k)}) + \langle O \rangle(\mu^{(k)}) q_m''(\mu^{(k)}) \\ \ldots \end{cases}$$

Alternatively we use a χ^2 minimization approach, i.e. we minimize

$$\chi^2_{generalized} = \sum_{k,j} (\partial^j_{\mu^j} R_{n,m}(\mu^{(k)}) - \partial^j_{\mu^j} \langle O \rangle(\mu^{(k)}))^2 / (\Delta \partial^j_{\mu^j} \langle O \rangle(\mu^{(k)}))^2$$

A first success: the Roberge-Weiss transition

Numerical set-up

As a first practical application, we consider $N_f = 2+1$ QCD in the high-temperature regime.

- We simulate highly improved staggered quarks (HISQ) in $N_f = 2+1$ QCD using $36^3 \times 6$ lattices
- Observables: $\chi^1_{B,Q} \equiv \frac{1}{Z}\frac{\partial Z}{\partial \hat{\mu}_{B,Q}}$ and their first $\hat{\mu}_B$-derivative
- 4 temperatures ($T = 195.0, 190.0, 185.0, 179.5\ MeV$)
- $O(10)$ imaginary chemical potentials in $[0, i\pi]$
- Enlarge interval to $[0, 2i\pi]$ by mirroring data using periodicity and parity

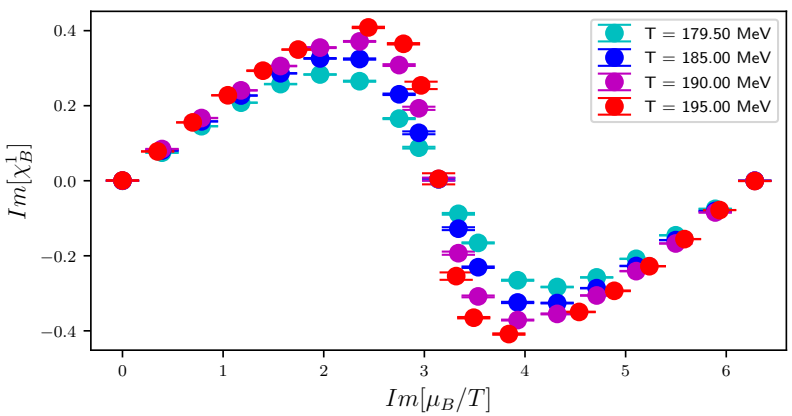

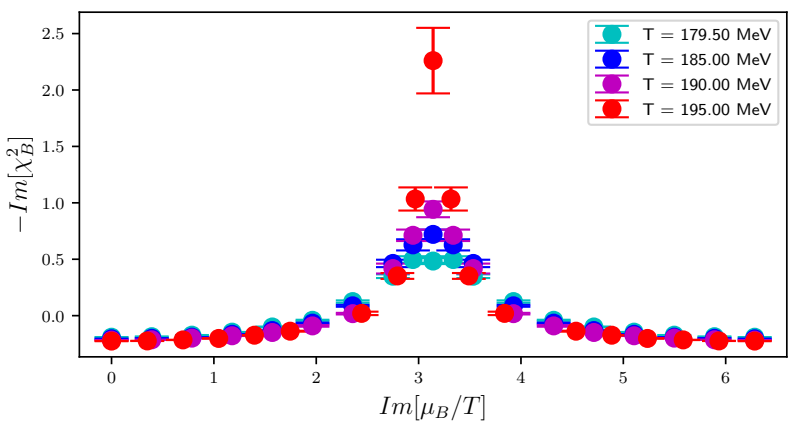

A first success: the Roberge-Weiss transition

Padé approximation

We approximate χ_B^1 with R_5^5 and R_{11}^{11} in the interval $[0, 2i\pi]$ using the χ^2 method:

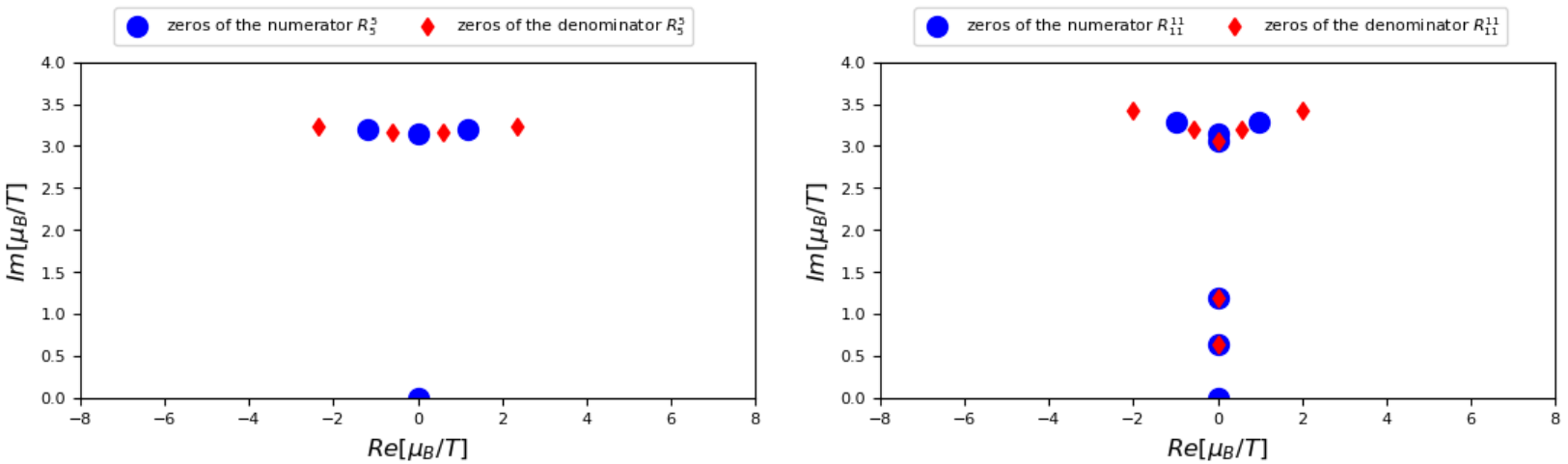

$\Rightarrow$ signature of branch cut singularities lying at $\mu_B/T = i\pi$

- Some zero/poles cancellations appear when we increase the order of the ansatz, but the location of the branch cut singularity is stable

  The location of the branch cut singularity is also stable with respect to the method used for building the approximation (χ^2 vs linearized system)

A first success: the Roberge-Weiss transition

Temperature dependence

$T = 179.5\ MeV$

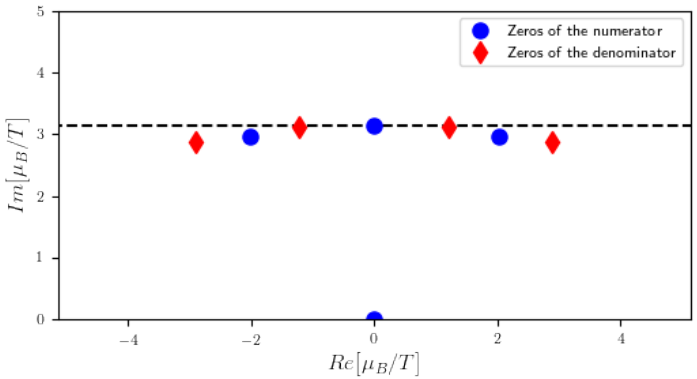

$T = 185.0\ MeV$

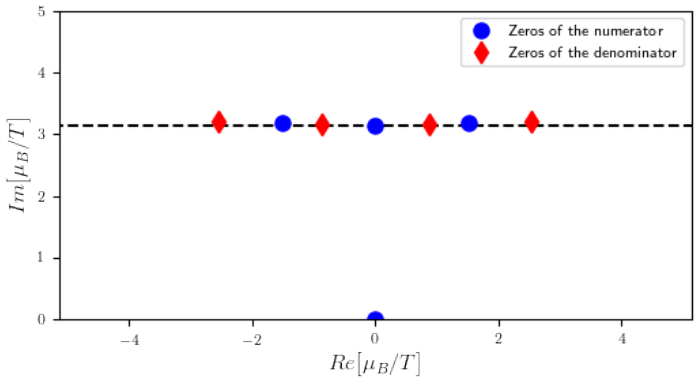

$T = 190.0\ MeV$

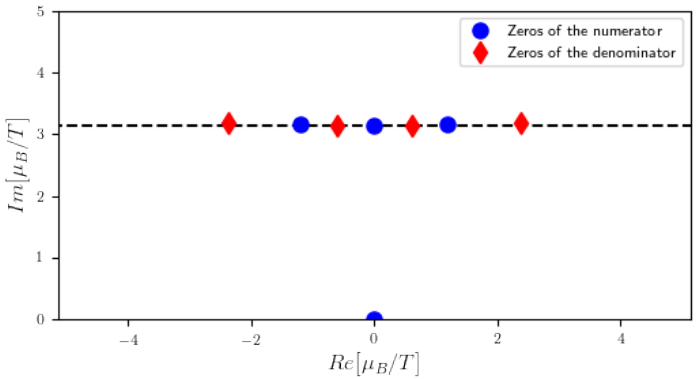

$T = 195.0\ MeV$

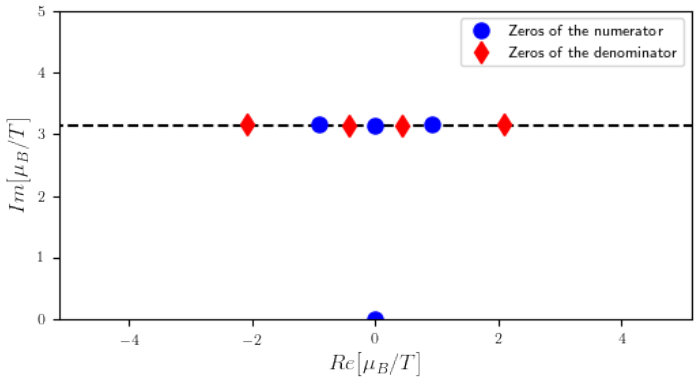

$\Rightarrow$ signature of branch cut singularities pinching the imaginary axis

A first success: the Roberge-Weiss transition

Temperature dependence

In summary,

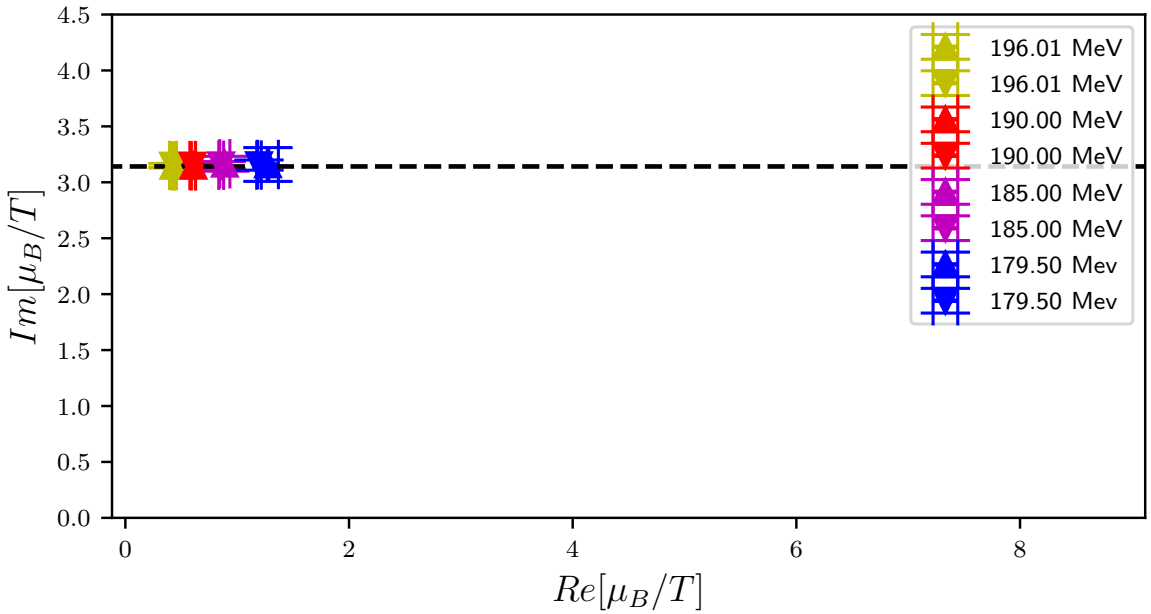

- For all temperatures we find singularities lying on $\hat{\mu}_B = i\pi$. We find compatible results using the Padé approximants for χ_B^1 (upward triangles) and χ_Q^1 (downward triangles).
- Are these the YLE singularities associated to the RW critical point?

A first success: the Roberge-Weiss transition

Scaling analysis

Theoretical expectations:

- Magnetic EoS: $M(h,t) = h^{\frac{1}{\delta}} f_G(z) + M_{reg}(h,t)$, where
  - $t = t_0^{-1} \frac{T_{RW}-T}{T_{RW}}$ and $h = h_0^{-1} \frac{\hat{\mu}_B - i\pi}{i\pi}$ are scaling fields
  - f_G is a scaling function depending only on the scaling variable $z = t/h^{\frac{1}{\beta\delta}}$
  - β and δ are the critical exponents [$3d, Z(2)$ universality class]
- We can solve $t/h^{\frac{1}{\beta\delta}} = z_c \equiv |z_c| e^{i\frac{\pi}{2\beta\delta}}$

  $$\rightarrow \hat{\mu}^R_{YLE} = \pm\pi \left(\frac{z_0}{|z_c|}\right)^{\beta\delta} \left(\frac{T_{RW}-T}{T_{RW}}\right)^{\beta\delta} \quad , \quad \hat{\mu}^I_{YLE} = \pi$$

Scaling analysis:

- We can fit the real part of the singularities using the ansatz:

  $$\hat{\mu}^R_{YLE} = a \left(\frac{T_{RW}-T}{T_{RW}}\right)^{\beta\delta} + b$$

  $\rightarrow$ estimate non-universal parameter T_{RW} from fit parameters

A first success: the Roberge-Weiss transition

Scaling analysis

- By fitting our data using $\beta\delta = 1.5635$ we obtain the estimate $T^{RW} = 207.08(35)\ MeV$. We can also estimate the continuum limit by a global fit of $N_t = 4, 6, 8$ data, assuming

$$a(N_t) = a_0 + a_2/N_t^2$$

$$T^{RW}(N_t) = T_0^{RW} + T_2^{RW}/N_t^2$$

- We find $T^{RW} = 211.1(3.1)\ MeV$, in good agreement with a previous work by the Pisa group

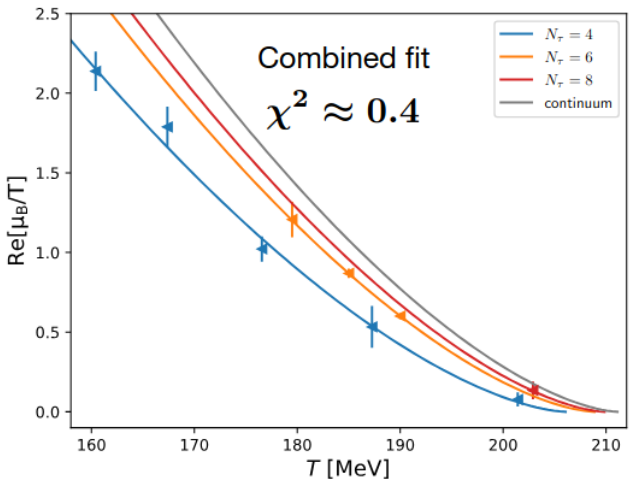

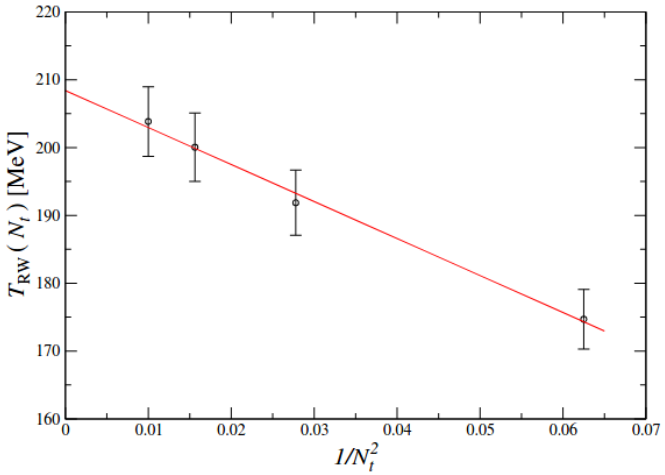

Phys.Rev.D 93 (2016) 7, 074504

The critical endpoint

Interval sensitivity

What happens at lower temperatures? At $T = 120\ MeV$ we find what looks like a second singularity when we restrict the fit interval from $[0, 2i\pi]$ to $[0, i\pi]$. This hints at the existence of a second critical point in a distinct region of the phase diagram.

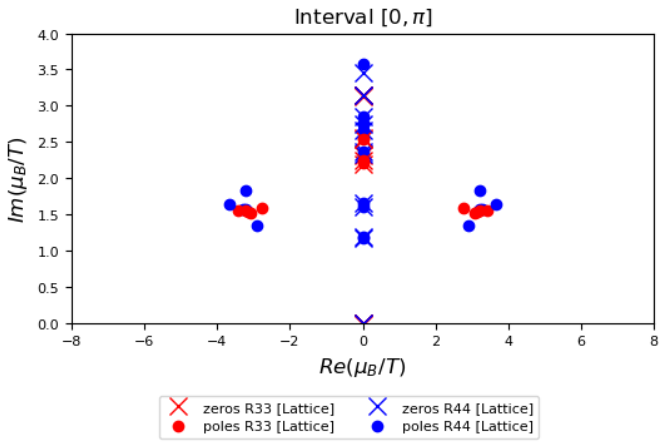

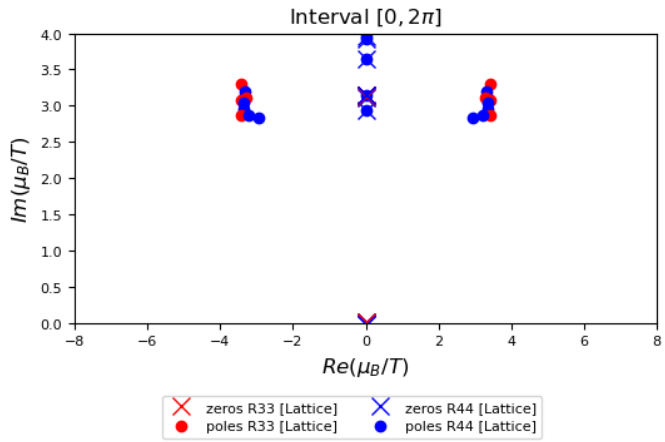

We can also look at the density plots of the solutions from several intervals of different length and center:

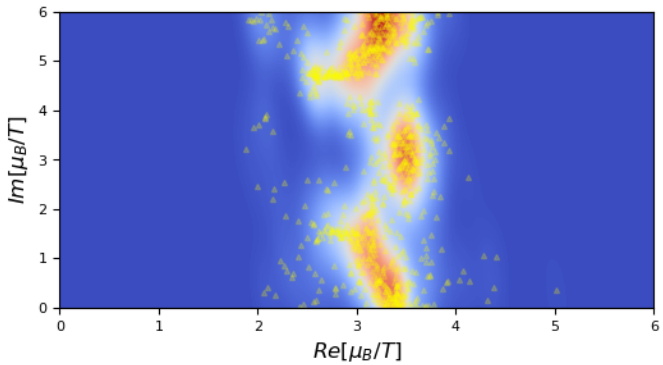

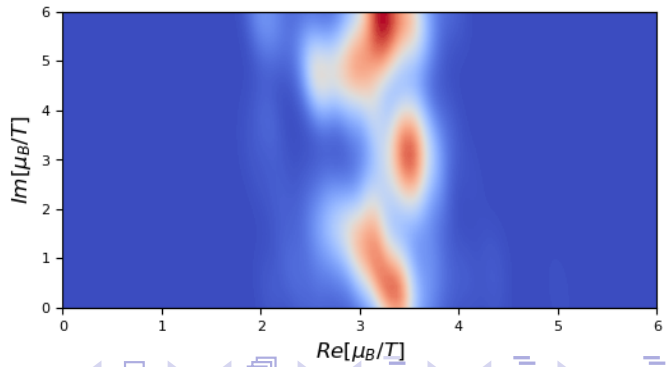

The critical endpoint

Interval sensitivity

For comparison, see the density plot at $T \sim T^{RW}$ [the dashed line is $i\pi$]

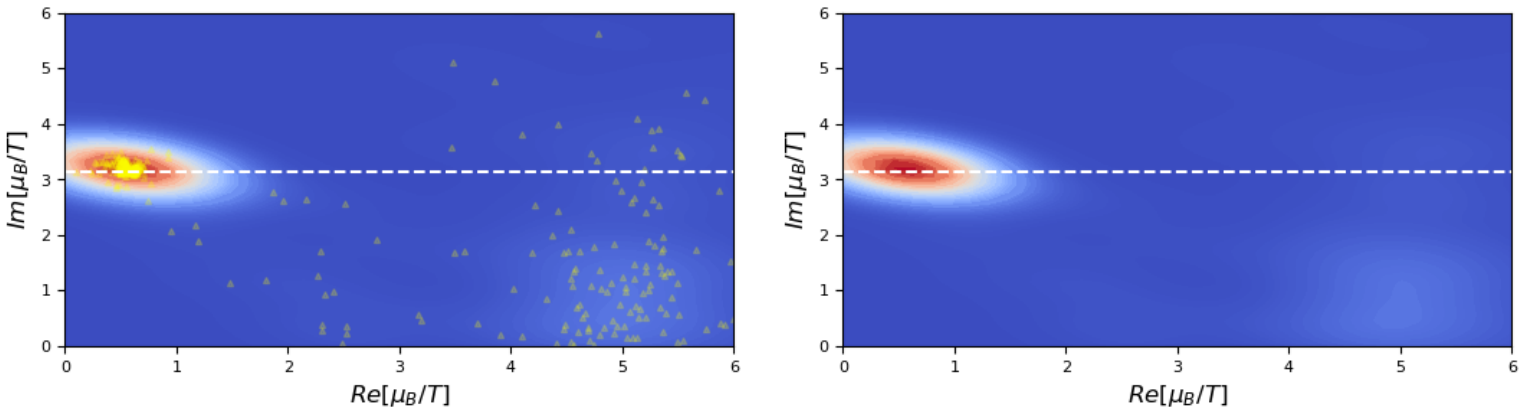

Poles are strongly localized in a single spot lying at $i\pi$, with possibly a second, faint and sparsely distributed spot which is barely noticeable.

We observe two regimes:

- High temperatures: almost no interval sensitivity, strong signal for the Roberge-Weiss YLEs
- Low temperatures: interval sensitivity, signal for a second kind of YLE singularity?

The critical endpoint

Interval sensitivity

- Notice that the interval sensitivity is something we have been aware for a while, from our experiments with toy models.

- 1-d Thirring model:

  Multi-point Padé approximation using an R_{10}^{10} ansatz with different fit ranges, $\mu_I \in [-2, 2], [-4, 4], [0, 4]$

  $\rightarrow$ we recover different singularities

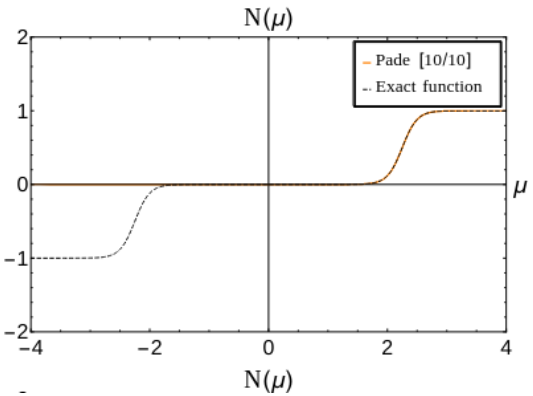

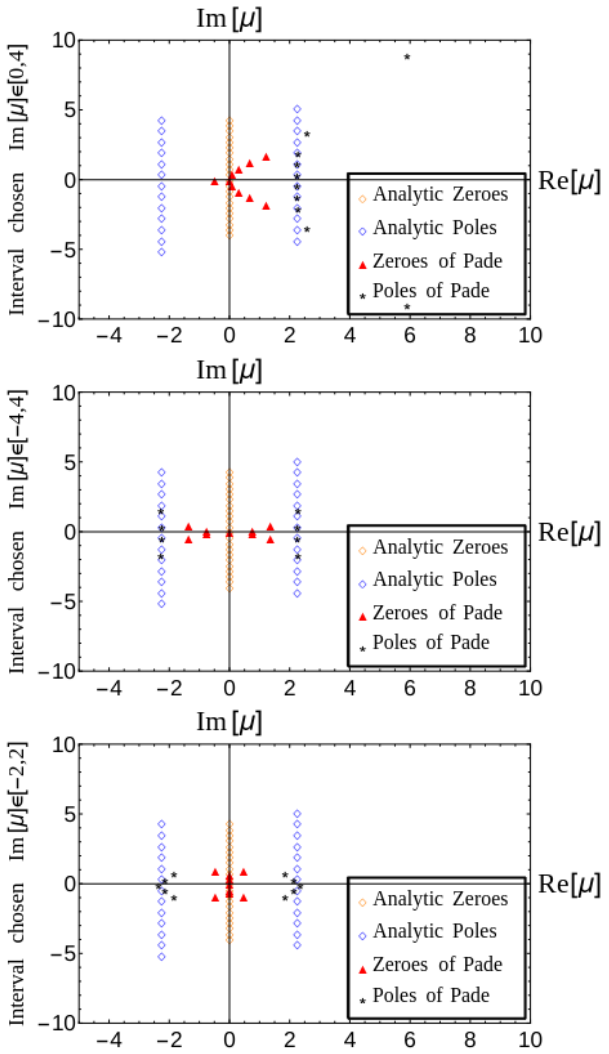

We performed new simulations in the low-temperature regime. Similar set-up:

- HISQ action, $N_f = 2 + 1$ flavours, $36^3 \times 6$ lattices
- Observable: $\chi^B_{1,2}(T, \mu_B)$
- 5 temperatures ($T = 120.0, 136.1, 157.5, 166.6\ MeV$)
- 10 imaginary chemical potentials between 0 and $i\pi$
- Observable extended to a larger interval $[-i\pi, i\pi]$ using periodicity and parity

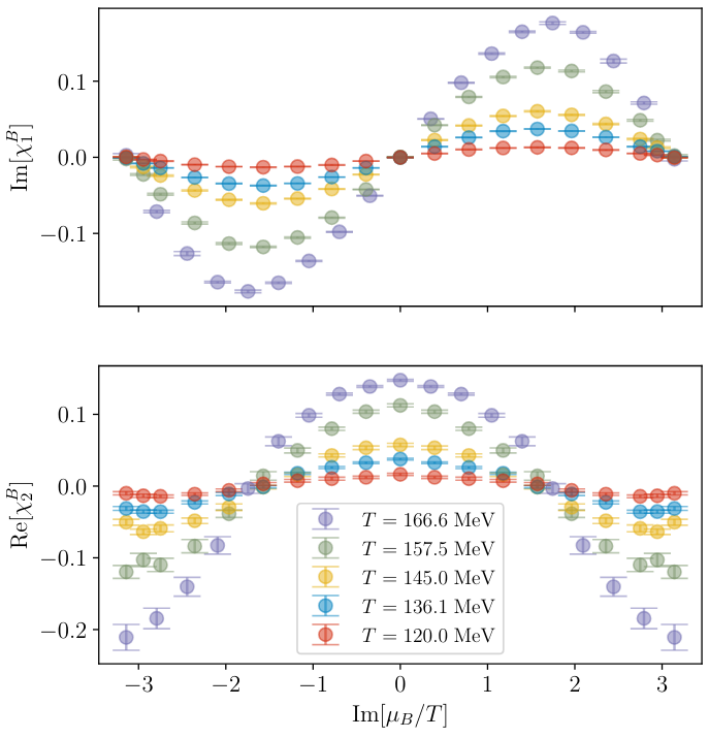

The critical endpoint

Numerical set-up

We need to account for the interval sensitivity $\rightarrow$ sliding window analysis

- Approximate $\chi^B_{1,2}(T, \mu_B)$ with a rational function
- Calculate zeros of the numerator and denominator
- Remove near cancelling pairs, keep poles in the first quadrant closest to the center of the interval
- Boostrap over the data
- Iterate over 55 intervals of varying length (from π to 2π) and center
- Perform scaling fits on randomly chosen intervals and collect the results for further analysis

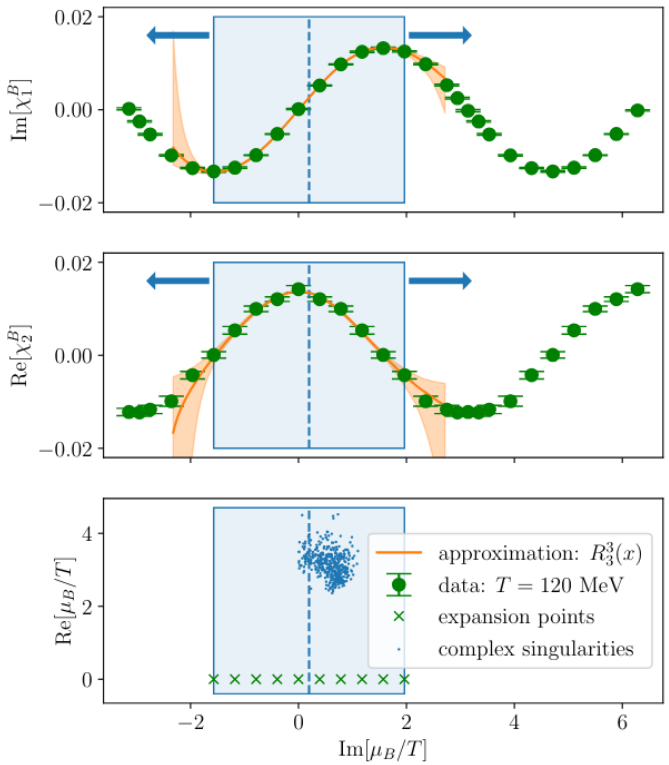

The critical endpoint

Scaling analysis

As for the scaling fits:

- The scaling fields for the CEP critical region are unknown. We can make use of a linear ansatz [Stephanov (2006), Basar (2021)]

$$t = \alpha_t(T - T_{CEP}) + \beta_t(\mu_B - \mu_{CEP})$$

$$h = \alpha_h(T - T_{CEP}) + \beta_h(\mu_B - \mu_{CEP})$$

- This leads to the scaling equations:

$$Re(\mu_{YLE}) = \mu_{CEP} + c_1(T - T_{CEP}) + c_2(T - T_{CEP})^2 + O((T - T_{CEP})^3)$$

$$Im(\mu_{YLE}) = c_3(T - T_{CEP})^{\beta\delta}$$

- The fit coefficient $c_1 = -\alpha_h/\beta_h$ is the inverse slope of the critical line at the critical point

Numerical results from $O(10^5)$ fits using an R_3^3 ansatz and 55 intervals:

- Histograms show a signal for a CEP candidate at

$$T^{CEP} = 105^{+8}_{-18}\ MeV$$

$$\mu_B^{CEP} = 422^{+80}_{-35}\ MeV$$

- Small differences between AIC weighted (orange) and non AIC weighted (blue)
- 1σ confidence ellipses from best scaling fit
- $\mu_B^{CEP}/T^{CEP} \sim 4$

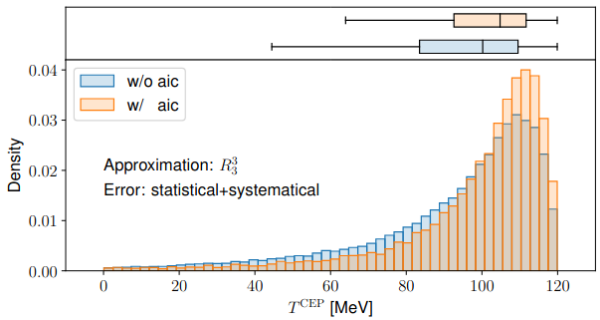

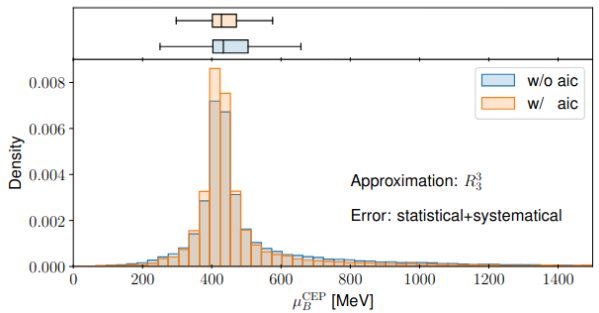

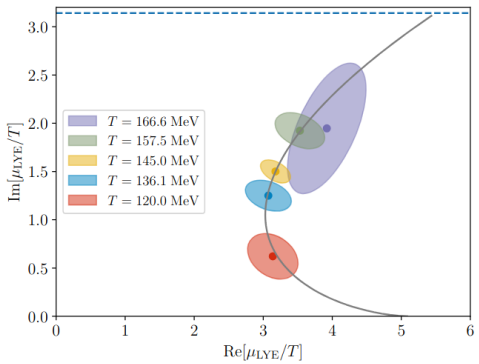

The analysis is subject to several sources of systematics that we should discuss.

Systematics from the Padé approximation:

- Interval chosen for the rational approximation
- Order of the rational approximation ansatz
- Others: approximation method? truncation order? observable?

Systematics from the lattice:

- Finite-size effects
- Cut-off effects

The critical endpoint

Systematics - interval sensitivity

The density plots show a temperature-dependent non-trivial structure.

Blob at $i\pi$ moving to lower $Re(\mu_B)$ as T increases. Second blob moving to larger $Re(\mu_B)$, $Im(\mu_B)$, either merging with first blob or becoming fainter.

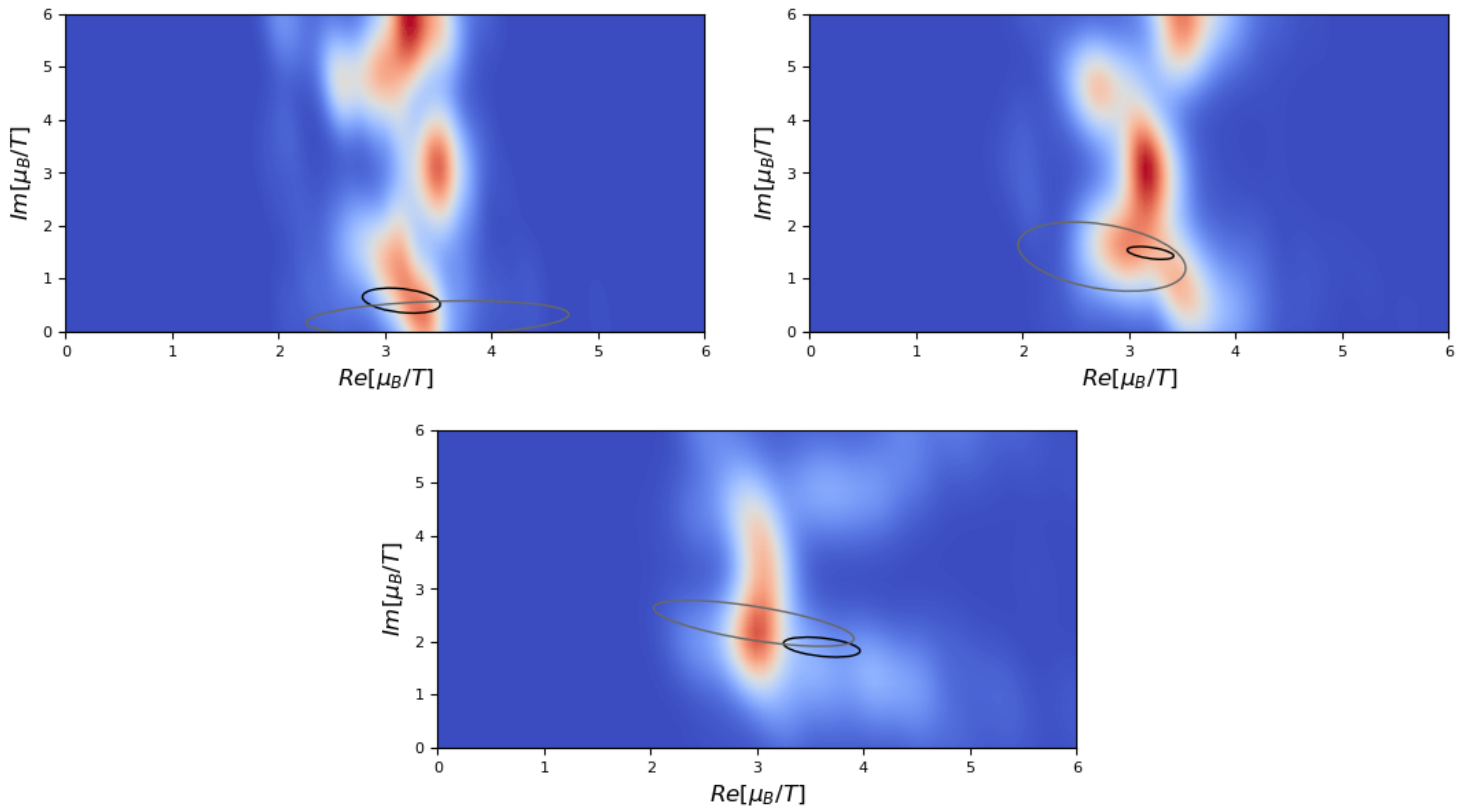

[$T = 120, 145, 157.5\ MeV$, clockwise order, 1σ confidence ellipses from best scaling fit for R_3^3 (black) / R_5^5 (grey)]

The critical endpoint

Systematics - interval sensitivity

We took the interval sensitivity into account by using a sliding window analysis. Moreover, we can also compare the results with and without the statistical bootstrap.

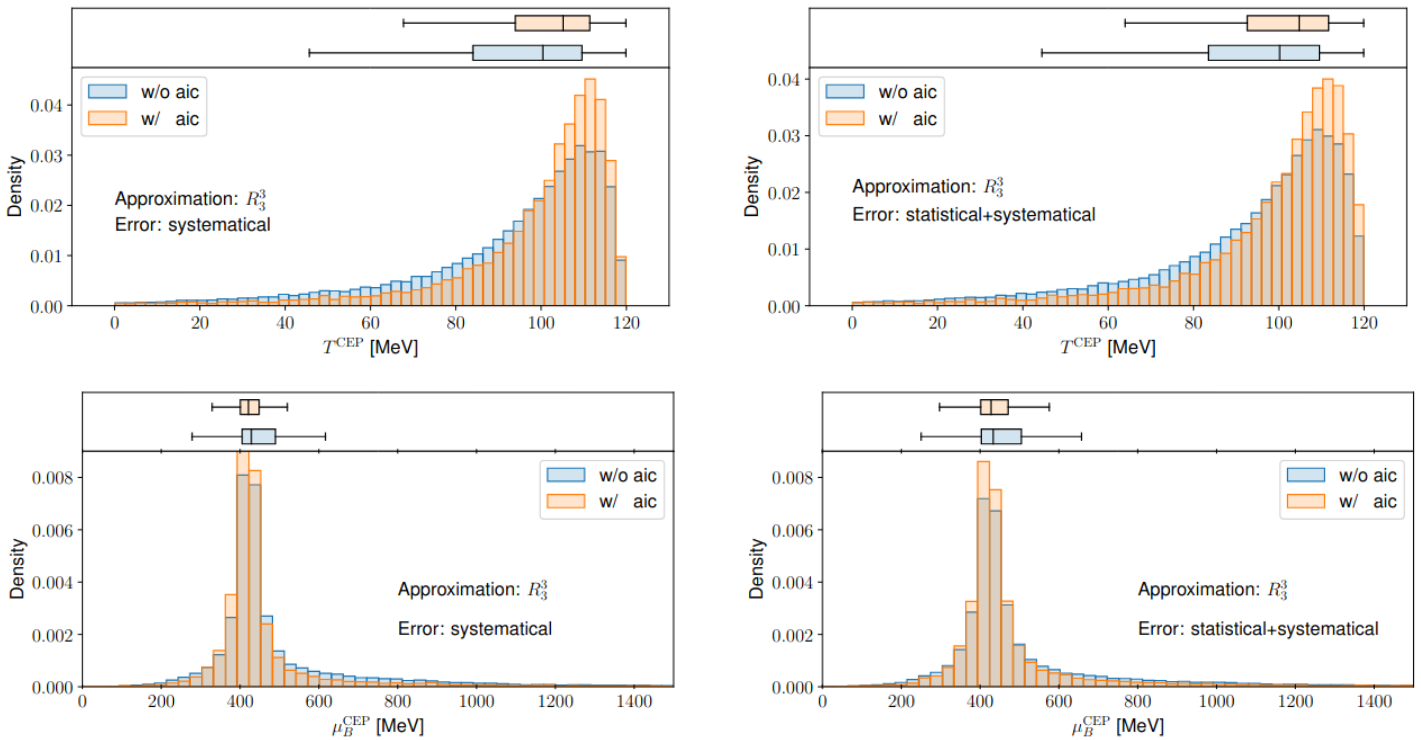

$\rightarrow$ statistical errors on $\mu_B^{CEP} \sim$ systematic uncertainty

The critical endpoint

Systematics - order of the ansatz

By visual inspection, we have seen that usually poles are stable with respect to the ansatz. Still, we can be more systematic and rerun the analysis with R^3_3, R^4_4 and R^5_5 approximants.

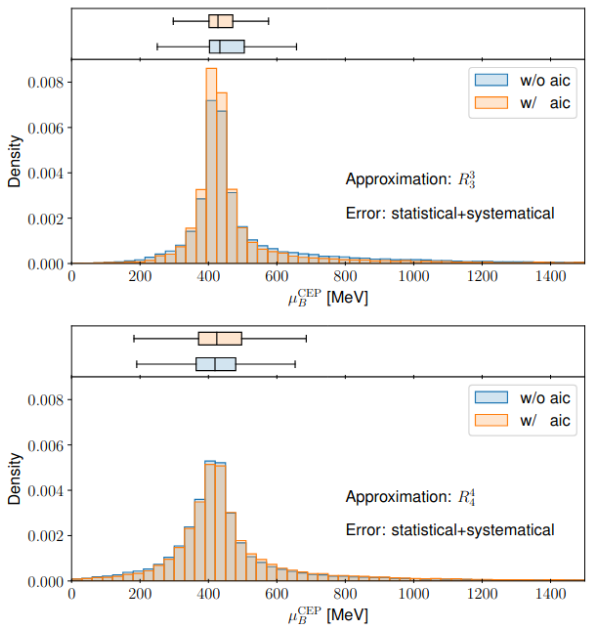

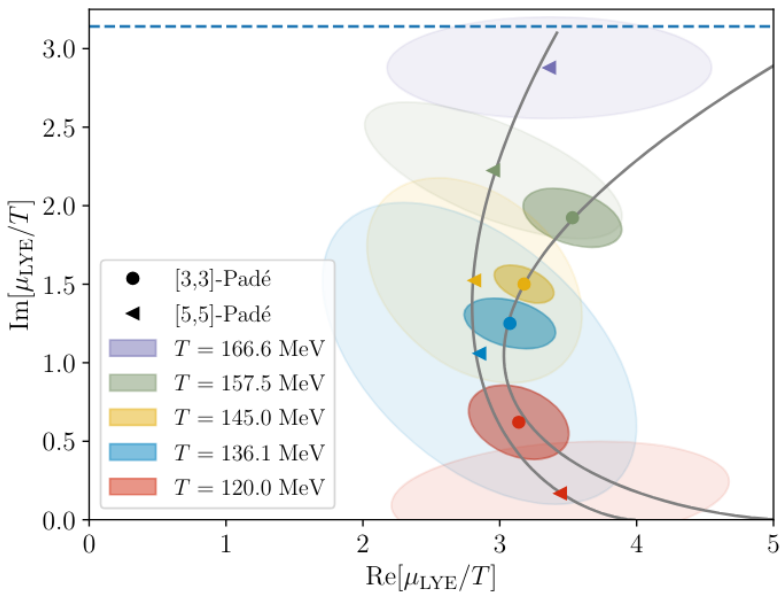

$\rightarrow$ The results for the CEP are compatible, the small difference between AIC weighted and non AIC weighted becomes even smaller. The YLEs from the best fits are compatible as well, but within very large errors.

The critical endpoint

Systematics - approximation method

Approximation method: zeros/poles structure from linear solver (left) vs χ^2_{gen} minimization (right) at $T = 145\ MeV$, for intervals $[0, i\pi]$ (top) and $[0, i2\pi]$ (bottom) $\rightarrow$ no difference (apart from cancelling pairs)

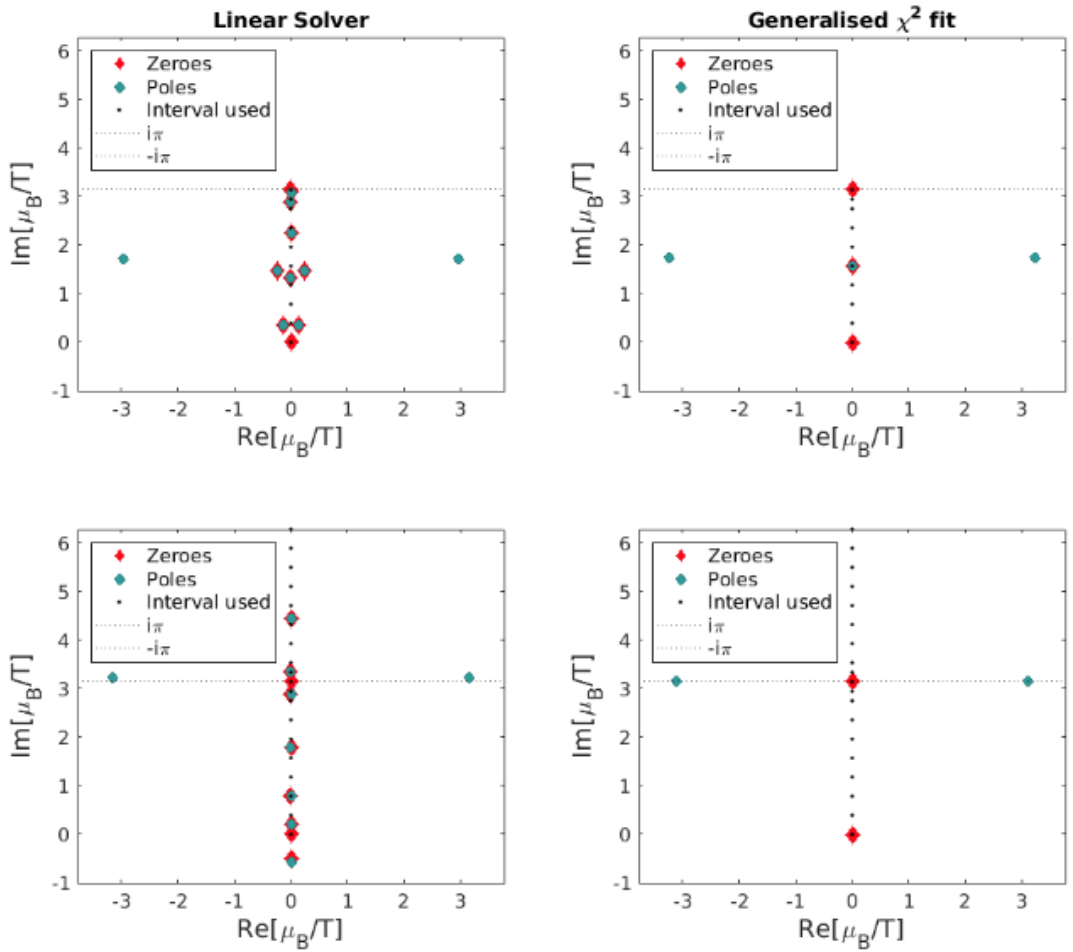

The critical endpoint

Systematics - truncation order

Truncation error: difficult to obtain a complete estimate because we don't have a good SNR for high order derivatives.

However, we can explore the effects of the truncation on the zeros-poles structure at $T = 157.5\ MeV$. At this temperature, the signal for χ_3^B is not entirely hidden by noise (and the effects of truncation seem small).

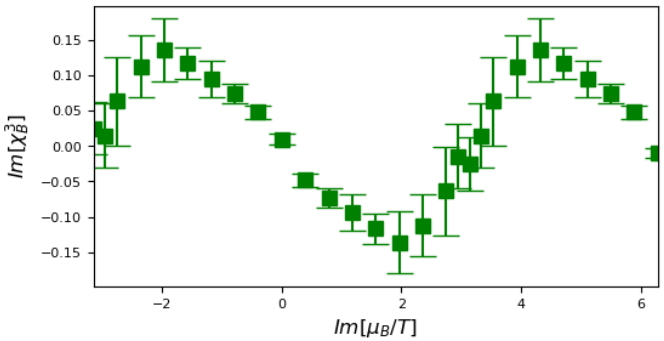

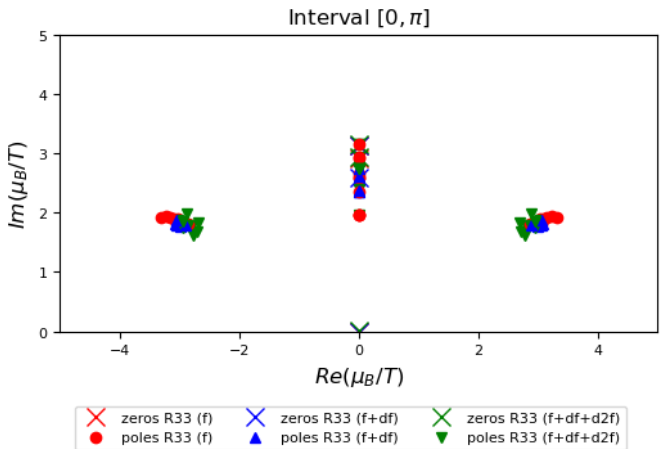

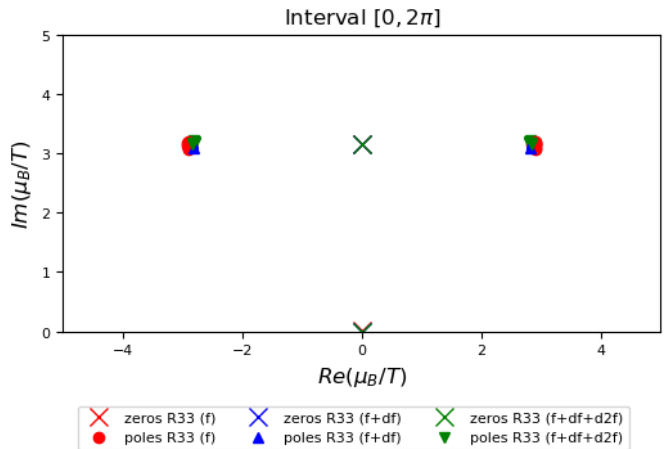

The critical endpoint

Systematics - observable

Observable: the rational approximations for χ^1_B and χ^1_Q at $T = 157.5$ MeV (top) and 120 MeV (bottom) yield compatible results for the poles.

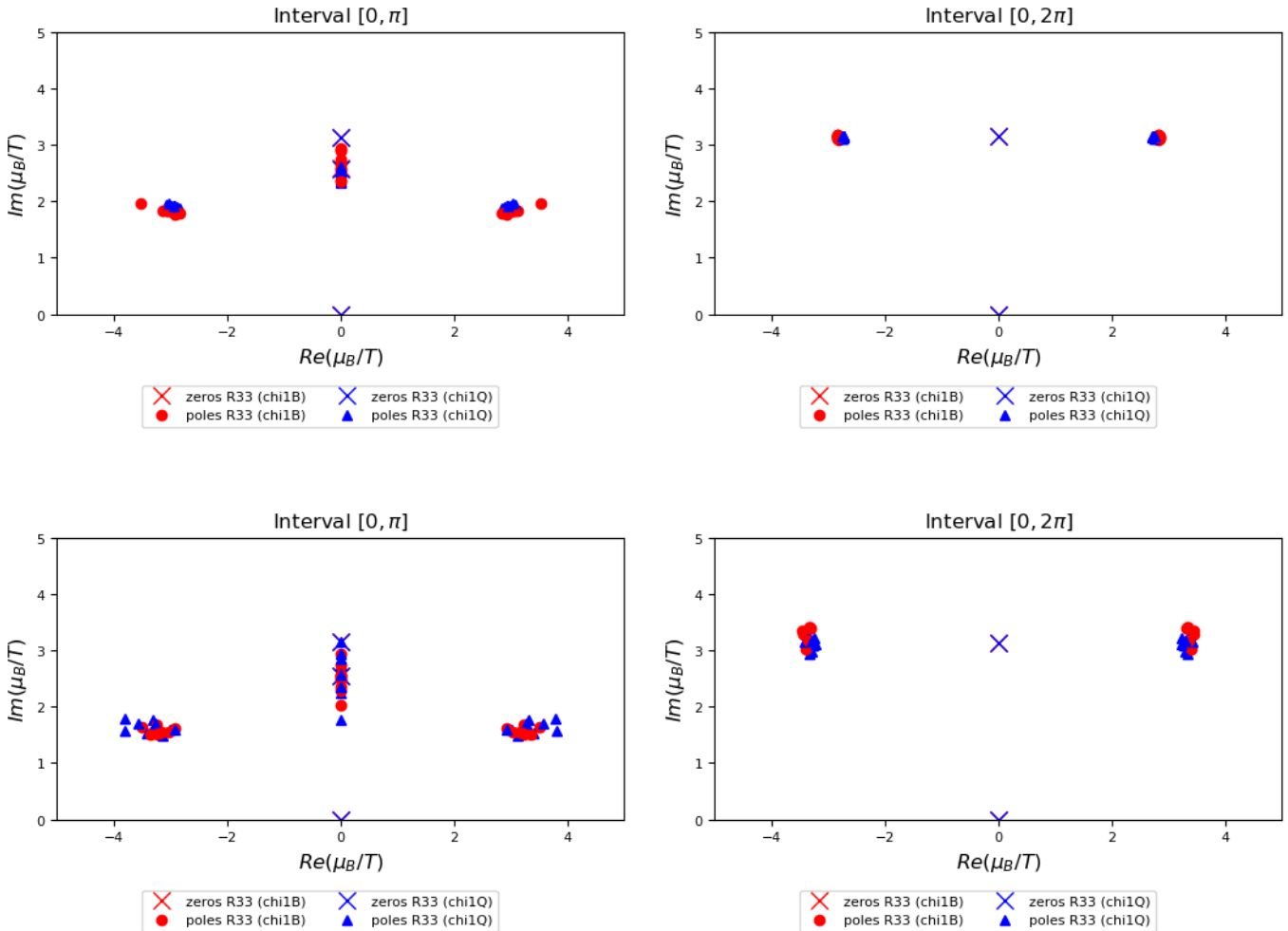

The critical endpoint

Numerical results

Numerical results from $O(10^5)$ fits using R_3^3, R_4^4, R_5^5 and 55 intervals:

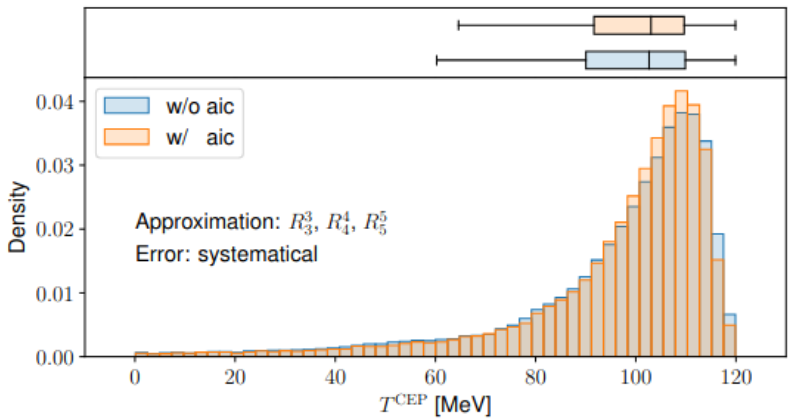

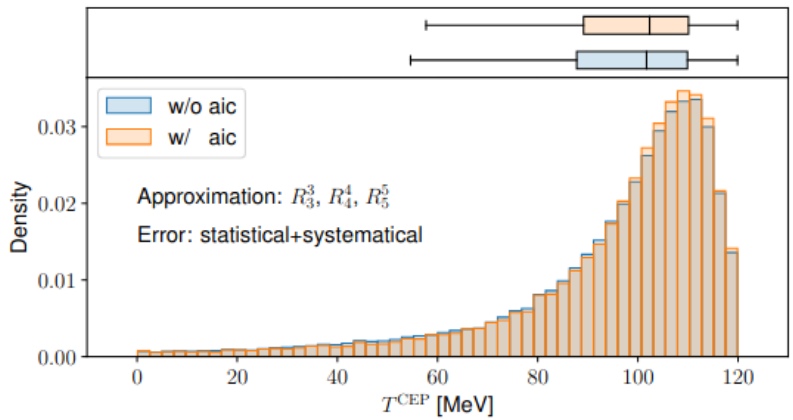

	$\mathbf{N_\tau = 6}$ multi-point Padé		
	T^{CEP} [MeV]	μ_B^{CEP} [MeV]	μ_B/T
best fit	111.9 ± 5.4	451.7 ± 72	4.04 ± 0.37
w/ AIC	$102.2 + 10.5 - 22.7$	$427.5 + 161.9 - 73.9$	$4.14 + 2.65 - 0.58$
w/o AIC	$101.7 + 10.9 - 24.1$	$424.2 + 147.9 - 77.3$	$4.11 + 2.58 - 0.59$
	c_1	c_2	c_3
best fit	-6.2 ± 7.6	0.15 ± 0.12	0.83 ± 0.14

The critical endpoint

Numerical results

Our current estimate is $T^{CEP} = 102^{+11}_{-23}\ MeV$ and $\mu_B^{CEP} = 428^{+162}_{-74}\ MeV$.

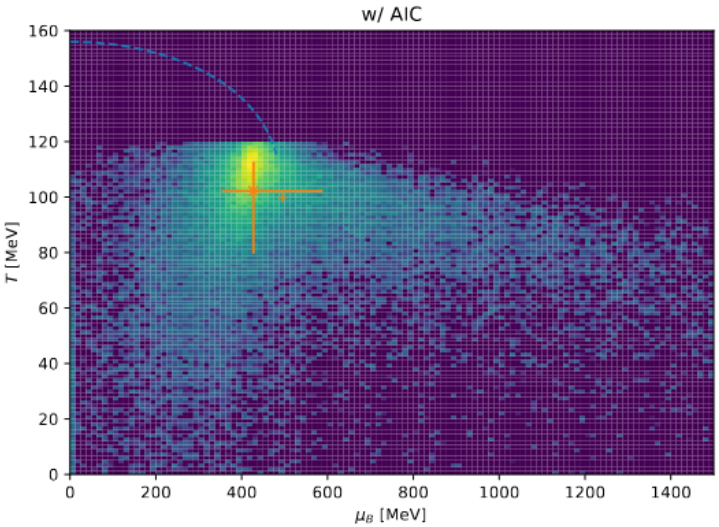

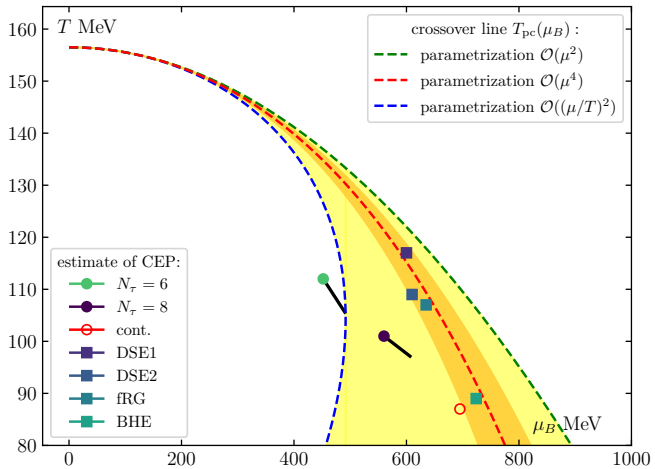

- Results in agreement with [Basar, arXiv: 2312.06952] and [Adam, arXiv: 2507.13254] (with some tension)
- Location of the CEP fits nicely with the chiral crossover line
- Parametrization for the chiral crossover line:
  1. $T_{pc}(\mu_B) = T_{pc}(0)\left[1 + k_2^B(\mu_B/T)^2 + k_4^B(\mu_B/T)^4\right]$
  2. $T_{pc}(\mu_B) = T_{pc}(0)\left[1 + \bar{k}_2^B(\mu_B/T_{pc}(0))^2 + \bar{k}_4^B(\mu_B/T_{pc}(0))^4\right]$

Parameters: $T_{pc}(0) = 156.5(1.5)$, $k_2^B = \bar{k}_2^B = -0.015(1)$, $k_4^B = \bar{k}_4^B = -0.0002(1)$

The critical endpoint

Systematics - lattice

- Finite-size effects: they are likely small. We use an $N_s/N_t = 6$ ratio, larger than most finite temperature simulations.
- Chiral and deconfinement observables below 170 MeV very close to the infinite volume limit.
- We estimate that the correction to the infinite volume scaling ansatz would amount to shifting T^{CEP} to larger values by ~ 10 MeV.

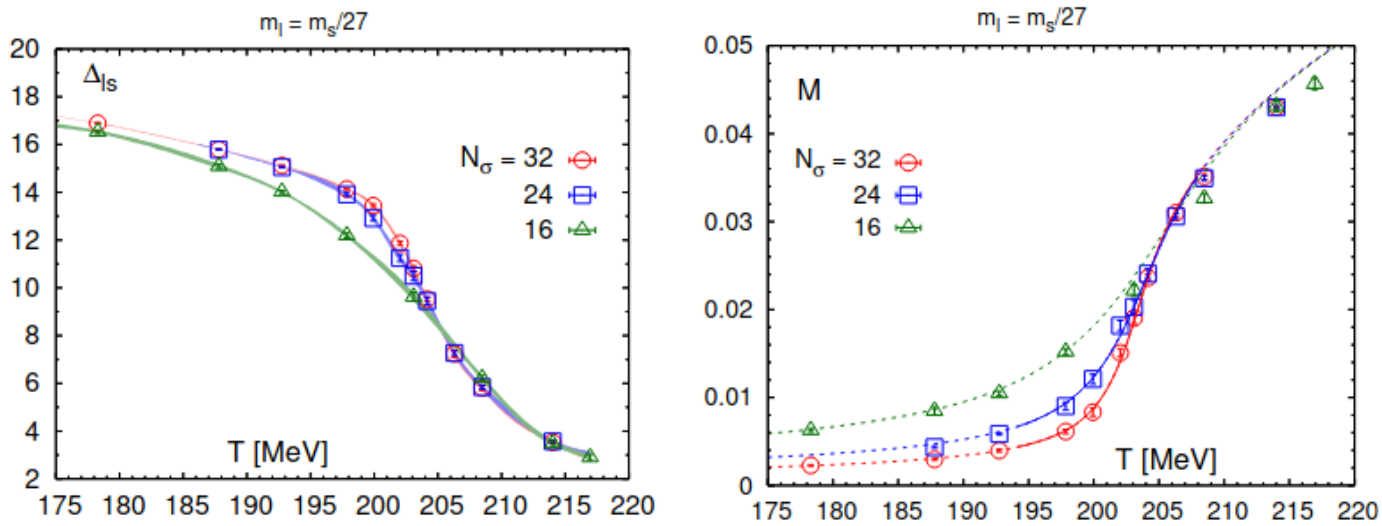

Figs. from [Cuteri arXiv: 2205.12707]

- Cut-off effects: we can try to compare our $N_t = 6$ results with the $N_t = 8$ results by HotQCD.

  Single-point Padé approximation for the 8-th order Taylor expansion of pressure, $\Delta p = \frac{p(T,\mu_B)}{T^4} - \frac{p(T,0)}{T^4} = \sum_{k=1}^{\infty} P_{2k}(T)\hat{\mu}_B^{2k}$

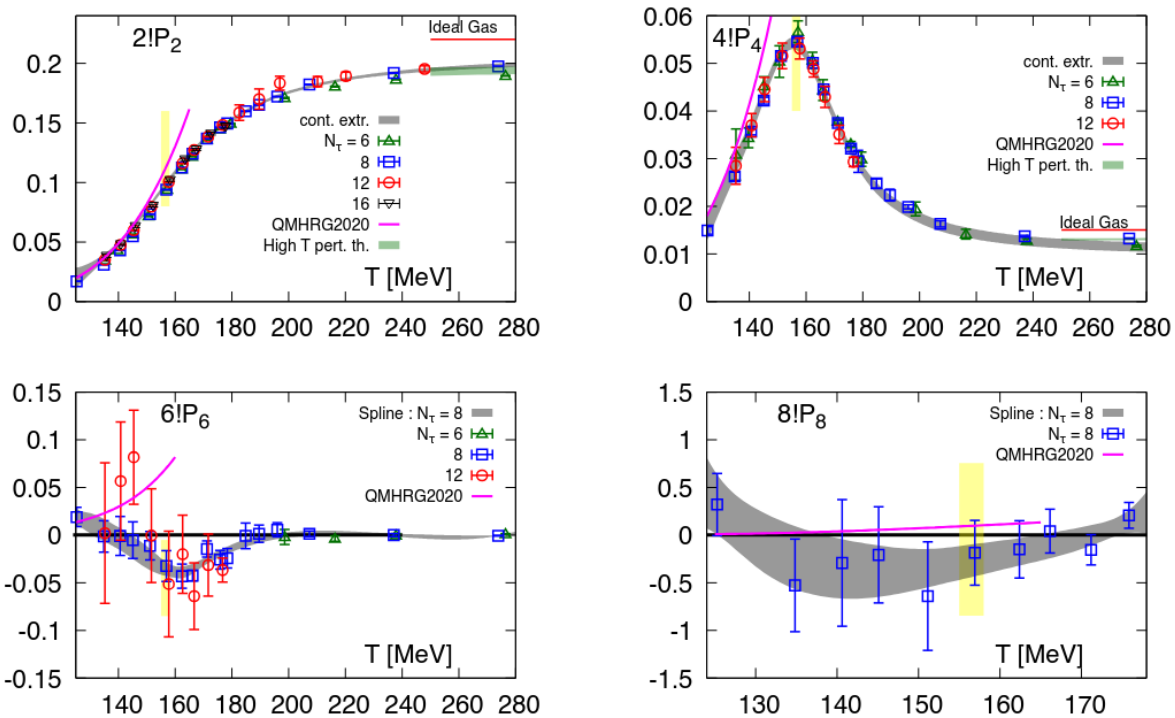

Fig. from [Bollweg, arXiv: 2212.09043]

The critical endpoint

Systematics - lattice

- After mapping the Taylor coefficients to an R_4^4 rational ansatz

$$R_4^4(\hat{\mu}_B) = \frac{P_2\hat{\mu}_B^2+(P_4+(P_2^2P_8)/P_4^2)\hat{\mu}_B^4}{1+((P_2P_8)/P_4^2)\hat{\mu}_B^2-(P_8/P_4)\hat{\mu}_B^4}$$

they calculate its complex poles and find poles approaching the real axis as T is decreased.

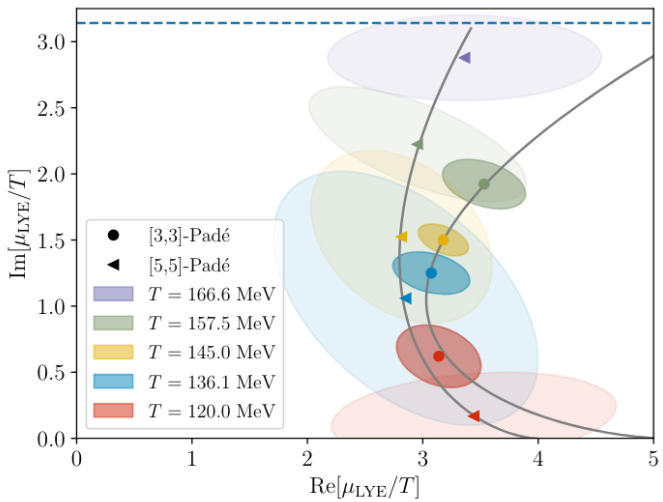

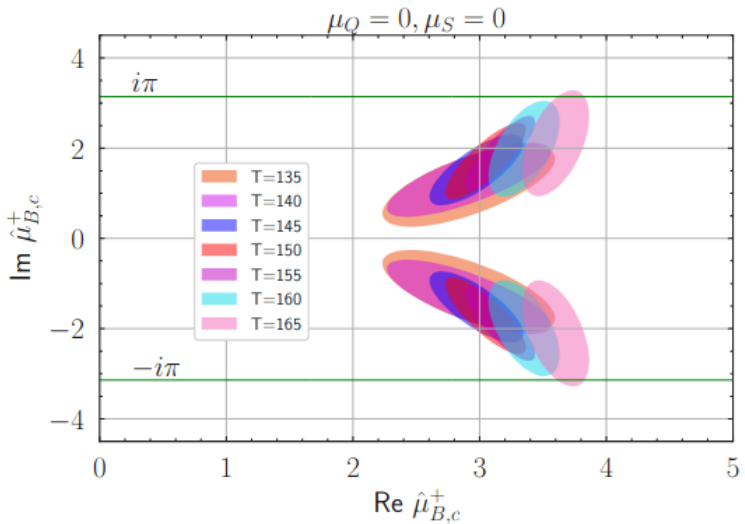

The critical endpoint

Systematics - lattice

- Results in agreement within errors. Difference in central values between $N_t = 6$ (green ellipse) and $N_t = 8$ (blue ellipse) could point to cutoff effects which shift μ_B towards ~ 650 MeV.
- However ellipses are still compatible within large uncertainties. Also different systematics involved (single-point vs multi-point Padé).

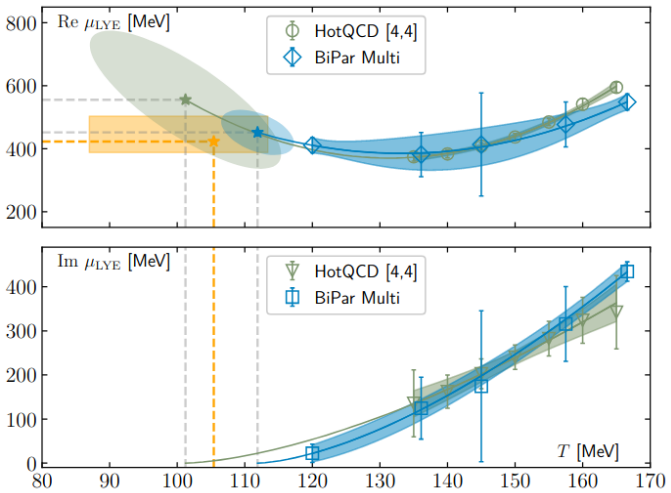

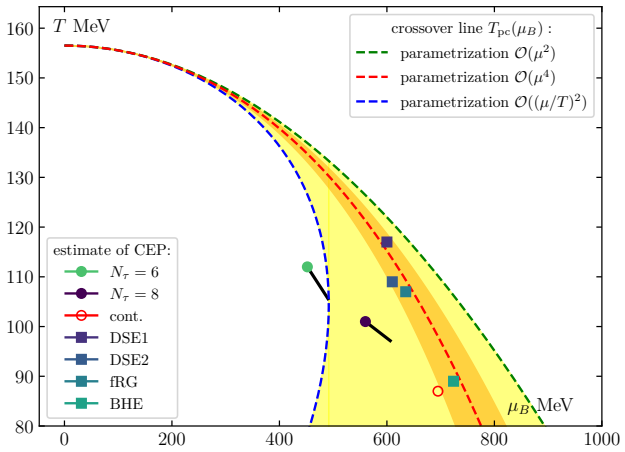

- But at the same time, [Basar arXiv: 2312.06952] also finds a larger central value for μ_B for $N_t = 8$.

Conclusions

To summarize:

- We have estimated the location of the QCD critical point by tracking the YLE singularities in the complex plane as a function of the temperature
- The analysis was performed using multi-point Padé approximations
- We have found $T^{CEP} = 102^{+11}_{-23}\ MeV$ and $\mu_B^{CEP} = 428^{+162}_{-74}\ MeV$
- These findings are consistent with other recent studies and with the current determination of the chiral crossover line
- These results are not extrapolated to the continuum yet
- A preliminary estimate of cutoff effects suggests a potentially larger $\mu_B^{CEP} \sim 650\ MeV$

Thank you for listening!

Backup slides

Comparison with the hadron resonance gas model

We can compare the Lattice data with *mock* data for the HRG model.

$\chi_B^{1,2}$: Lattice (green) vs HRG (black)

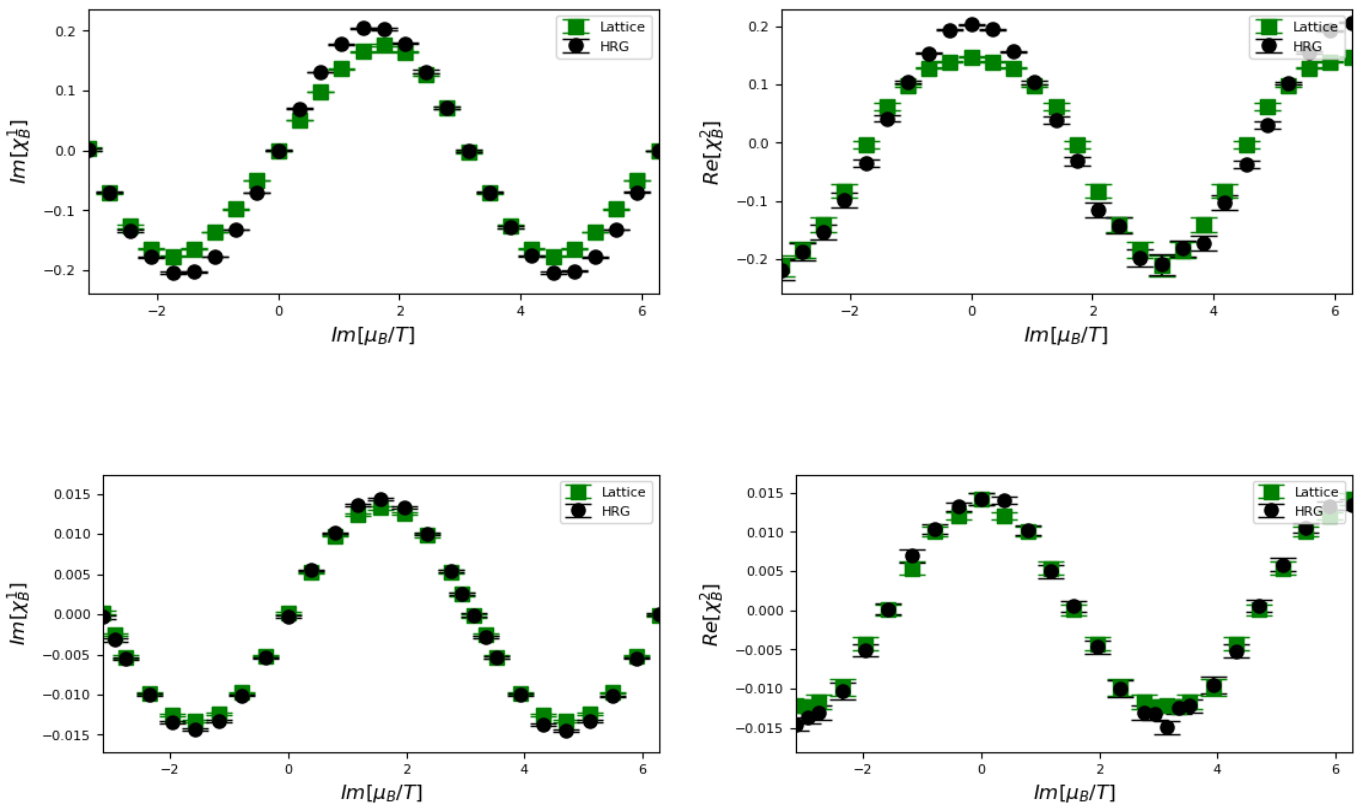

[$T = 166.7$ *MeV* (top), 120.0 *MeV* (bottom)]

Backup slides

Comparison with the hadron resonance gas model

Zeros-poles structure for $[0, \pi]$ and $[0, 2\pi]$ at 166.7 MeV:

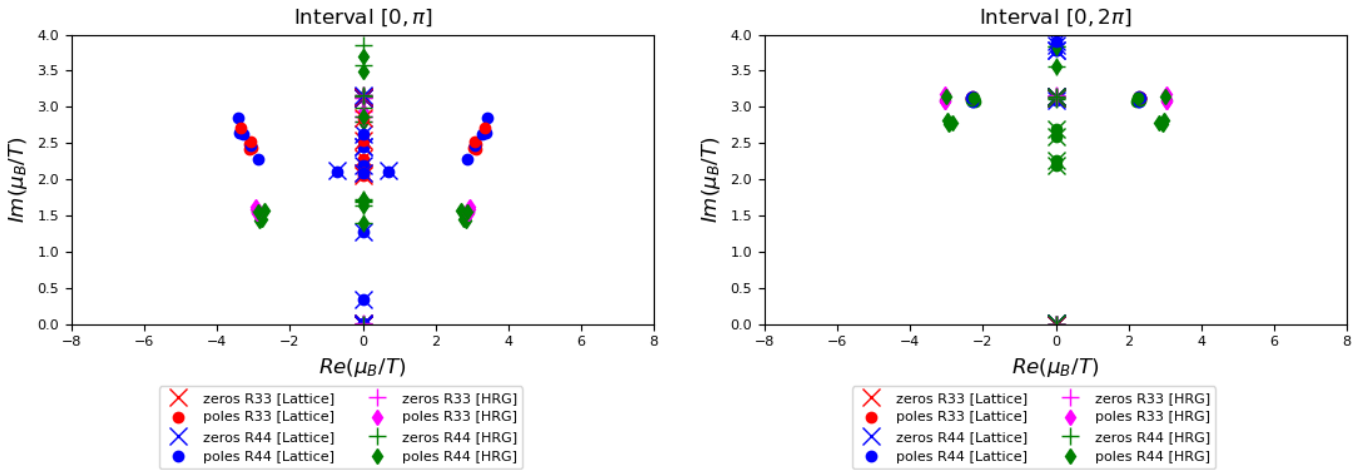

Zeros-poles structure for $[0, \pi]$ and $[0, 2\pi]$ at 120 MeV:

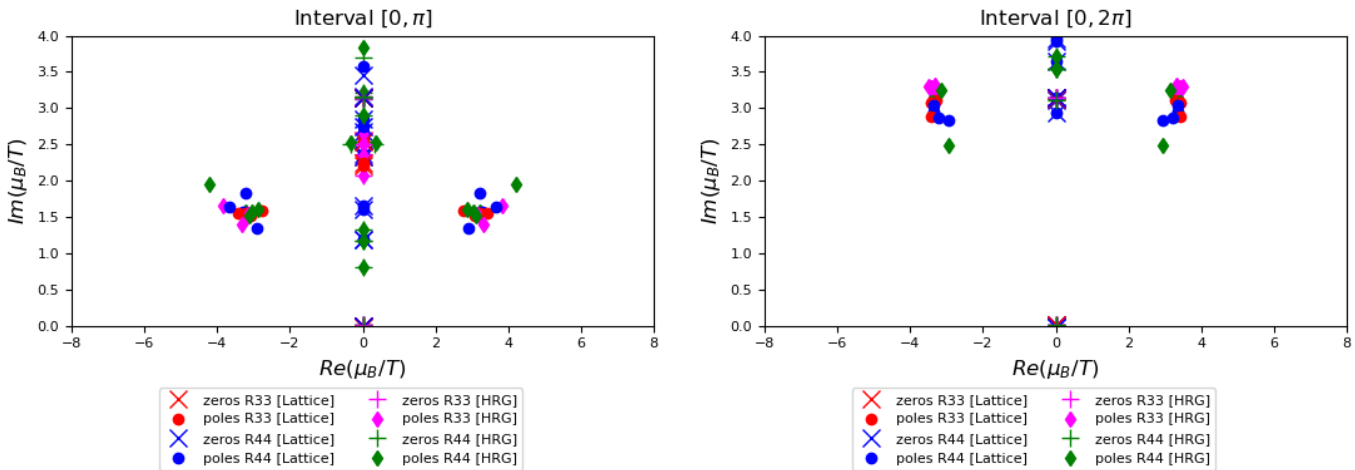

Backup slides

Comparison with the hadron resonance gas model

$\Delta\chi_B^1 = \chi_B^{1,Lattice}$ - $\chi_B^{1,HRG}$ (at $T = 120$ MeV)

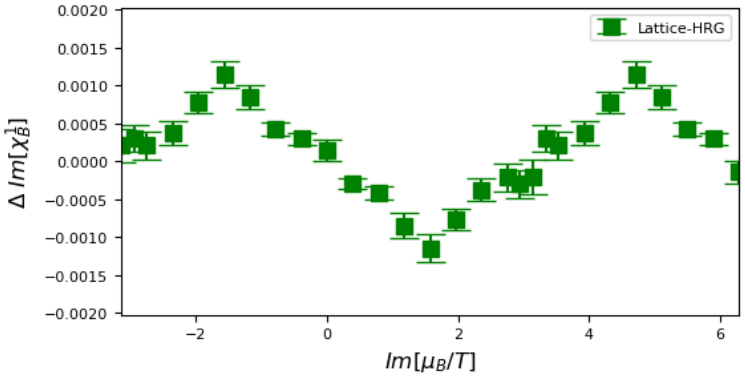

Density plots: Lattice (left) vs HRG (right)

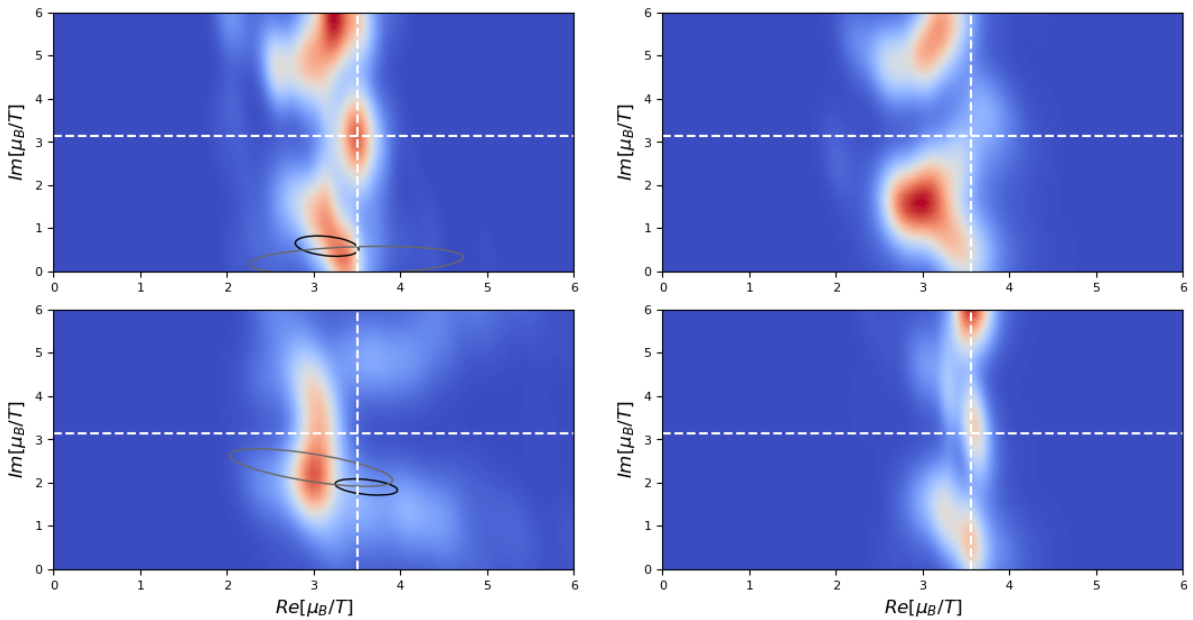

[$T = 120.0$ MeV (top), 157.5 MeV (bottom)]

Backup slides

Comparison with the hadron resonance gas model

- Corrections to the HRG model become small at low temperature
- At $T = 120\ MeV$, corrections to the observables are still statistically significant
- However the zeros-poles structure of Lattice and HRG data are compatible within errors
- Will (very) high-order Taylor coefficients be required for analyses at lower temperatures?